Advances in Nano Research, *Vol. 5 No. 3 (2017) 203-214*
DOI: https://doi.org/10.12989/anr.2017.5.3.203

Evolution pathway of CZTSe nanoparticles synthesized by microwave-assisted chemical synthesis

Odín Reyes [1a], Mónica F. Sánchez [1], Mou Pal [2], Jordi Llorca [3] and P.J. Sebastian [*1]

[1] *Instituto de Energías Renovables-UNAM, Temixco, Morelos, 62580, México*
[2] *Instituto de Física, BUAP, Puebla, 72570, Mexico*
[3] *Institute of Energy Technologies and Barcelona Research Center, in Multiscale Science and Engineering, Universitat Politècnica de Catalunya, EEBE, Eduard Maristany 10-14, 08019 Barcelona, Spain*

(*Received December 04, 2016, Revised July 04, 2017, Accepted August 01, 2017*)

Abstract. In this study we present the reaction mechanism of $Cu_2ZnSnSe_4$ (CZTSe) nanoparticles synthesized by microwave-assisted chemical synthesis. We performed reactions every 10 minutes in order to identify different phases during quaternary CZTSe formation. The powder samples were analyzed by x-ray diffraction (XRD), Raman spectroscopy, energy dispersive spectroscopy (EDS), X-ray photoelectron spectroscopy (XPS) and transmission electron microscopy (TEM). The results showed that in the first minutes copper phases are predominant, then copper and tin secondary phases react to form ternary phase. The quaternary phase is formed at 50 minutes while ternary and secondary phases are consumed. At 60 minutes pure quaternary CZTSe phase is present. After 60 minutes the quaternary phase decomposes in the previous ternary and secondary phases, which indicates that 60 minutes is ideal reaction time. The EDS analysis of pure quaternary nanocrystals (CZTSe) showed stoichiometric relations similar to the reported research in the literature, which falls in the range of Cu/(Zn+Sn): 0.8-1.0, Zn/Sn: 1.0-1.20. In conclusion, the evolution pathway of CZTSe synthesized by this novel method is similar to other synthesis methods reported before. Nanoparticles synthesized in this study present desirable properties in order to use them in solar cell and photoelectrochemical cell applications.

Keywords: CZTSe; solar cell; nanoparticles; microwave-assisted chemical synthesis

1. Introduction

Chalcopyrites are considered as one of the most promising absorber materials for thin film solar cells (Bhattacharya *et al*. 1998). $Cu(InGa)(S,Se)_2$ (CIGS) based solar cells have achieved a record efficiency of 22.6% (Jackson *et al*. 2016). However, the scarcity and high cost of In and Ga are limitations for large scale production (Mitzi *et al*. 2011). $Cu_2ZnSnS_xSe_{(1-x)4}$ (CZTSSe) are materials that avoid these limitations, which make them a potential candidate for large scale production of thin film solar cells. CZTSSe materials present outstanding optical and electrical properties; p-type conductivity, large absorption coefficient ($> 10^4$ cm^{-1}) and a tunable band gap of 0.85 to 1.65 eV (Zhou *et al*. 2013), which is close to the optimal value for single-junction solar cells as predicted

∗Corresponding author, Ph.D., E-mail: sjp@ier.unam.mx
[a] Ph.D. Student, E-mail: odrev@ier.unam.mx

http://www.techno-press.org/?journal=anr&subpage=5 ISSN: 2287-237X (Print), 2287-2388 (Online)

theoretically (Shockley and Queisser 1961).

In this study we propose the microwave assisted chemical synthesis (MACS) because of its advantages over the conventional solvothermal process. These are simplicity, fastness and energy efficiency, these advantages are due to the direct excitation of intramolecular and intermolecular chemical bonds. MACS has proved to be able to synthesize inorganic photovoltaic materials, such as CZTS, $CuInSe_2$, $CuInTe_2$, $CuInS_2$, ZnSe, Cu_2S, CdS, CdSe, ZnS, ZnSe and CdTe (Flynn *et al*. 2012, Grisaru *et al*. 2003, Gardner *et al*. 2008, Qian *et al*. 2006, Wang *et al*. 2012, Panda *et al*. 2006, Washington and Strouse 2008).

CZTSSe-based thin film solar cells have reached maximum efficiency of 12.6% (Wang *et al*. 2014). These materials have been synthesized by techniques like evaporation (Shao *et al*. 2012), sputtering (Zoppi *et al*. 2009), mechanosynthesis (Shyju *et al*. 2015), solvothermal synthesis (Du *et al*. 2012), spin coating (Todorov *et al*. 2010), chemical bath deposition (Wangperawong *et al*. 2011), doctor blade (Qin-Miao *et al*. 2012), electrodeposition (Jeon *et al*. 2011), and solid-state reaction (Wibowo *et al*. 2010). The champion CZTSSe based solar cell has been deposited by spin coating, using hydrazine based precursor solution followed by selenization process (Wang *et al*. 2014). However, hydrazine is an explosive, hepatotoxic and carcinogenic solvent (Roe *et al*. 1967).

In order to follow the green chemistry principles, it is necessary to develop a complete environmentally friendly process, involving the use of non-toxic solvents and reactants, which do not decompose during the synthesis process producing toxic or dangerous gases. Some solvents or mixture of solvents used for CZTSe synthesis are: isophorondiamine (Lee *et al*. 2013), triethylene glycol (Li *et al*. 2011), triethylenetramine (Zhou *et al*. 2013), ethylenediamine and polyvinyl-pyrrolidone (Du *et al*. 2012), oleylamine (Rath *et al*. 2012), isophorondiamine and trioctylphosphine (Shei and Lee 2013) and triethanolamine (Liu *et al*. 2011). From these solvents only triethylene glycol and triethanolamine can be considered as non-toxic. Because of this, triethanolamine was used in this study as solvent.

2. Experimental details

We performed a systematic study on the synthesis of CZTSe by MACS, analyzing the effect of reaction time on the crystalline structure and chemical composition of CZTSe nanocrystals, in order to identify the reaction mechanism. In previous study we described the optimum conditions for reactant concentration and proportion of water and TEA as solvent (Vallejo *et al*. 2016). The precursor solution was prepared by adding 1.0 mmol of copper (II) chloride dihydrate ($CuCl_2 \cdot 2H_2O$), 0.5 mmol of tin (II) chloride dihydrate ($SnCl_2 \cdot 2H_2O$), 0.5 mmol of zinc nitrate hexahydrate ($ZnNO_3 \cdot 6H_2O$) and 2.0 mmol of elemental selenium powder (Se) into 6.8 ml of triethanolamine (TEA) and 3.2 ml of deionized water. The solution was stirred at 100℃ for 30 minutes in order to dissolve the reactants. Reactions were performed in a microwave oven (Anton Paar Synthos 3000 operating at 2.45 GHz), which was programmed at 240℃ for different reaction times, from 0 to 90 minutes, using a 5 min heating ramp at 600W, besides a security limit of maximum pressure of 60 psi was set. At the end of the reaction a black precipitate was obtained which was separated by centrifugation and washed several times with deionized water and ethanol. Then the product was dried in an oven for 3 to 5 h at 60℃ to obtain the dry powder, which was used for further characterization.

The crystal structure of the nanoparticles obtained was characterized by powder X-ray difraction (XRD), using a Rigaku diffractometer, with Cu-Kα radiation, λ = 1.5406 Å, in the 2θ

range of 10-100°. Raman spectroscopy was used in order to confirm the formation of the quaternary CZTSe phase and discard the presence of other secondary phases. Raman spectra of the samples were recorded with a JobinYvon RAM HR800 Raman spectrometer equipped with an Olympus BX41 microscope and a charge-coupled device detector. The 632.8 nm emission of a He-Ne laser was used as the excitation source. Elemental composition was analyzed by X-ray energy dispersive spectroscopy (Oxford Instruments) attached to a Hitachi SU1510 scanning electron microscope (SEM). X-ray photoelectron spectroscopy (XPS) was performed using a SPECS system equipped with an Al anode XR50 source operating at 150 mW and a Phoibos 150 MCD-9 detector. The pass energy of the hemispherical analyzer was set at 25 eV and the energy step was set at 0.1 eV. The binding energy (BE) values were referred to the C 1s peak at 284.8 eV. High-resolution transmission electron microscopy (HRTEM) was accomplished with a JEOL J2010F instrument equipped with a field emission electron source and operated at 200 kV. Samples were dispersed in alcohol and a drop of the suspension was placed over a grid with holey-carbon film.

3. Results and discussion

Fig. 1 presents the x-ray diffraction patterns of nanocrystals obtained at different reaction times, from 0 to 90 minutes. The 0 minute case includes the 30 minutes dissolving time at 100℃ and the 5 minutes of ramp heating at 600 W. We can observe that 0 minute case predominates secondary phases, the peaks diffracted at 2 theta values of 26.6 and 31.1° correspond to (111) and (200) planes of $Cu_{1.8}Se$ (PDF 01-071-4324), the peaks diffracted at 2 theta values of 28.0, 29.7, 33.1, 34.0, 38.7, 41.9, 46.0, 48.6, 52.9, 53.9 and 60.7° correspond to (011), (101), (111), (120), (210), (121), (211), (002), (002), (221), (131) and (122) planes of $CuSe_2$ (PDF 01-071-0046), the peak diffracted at 2 theta value of 50.0° corresponds to (110) plane of CuSe (PDF 01-070-8589) and the peaks diffracted at 2 theta values of 41.9, 48.6 and 56.0° correspond to (410), (122) and (600) planes of Se (PDF 00-051-1389), the peaks around 27.2, 45.3 and 53.8° are really hard to associate to a particular phase due to diffraction of secondary, ternary and quaternary phases. We can conclude that at the beginning of the reaction mechanism there is a tendency to form copper selenide secondary phases, this tendency to form copper selenide phases is explained considering the Pearson classification of ions as hard or soft acids/bases depending on their polarizability, oxidation state and electronegativity (Ahmadi *et al*. 2012). Based on this classification Cu ions are classified as soft acids, while Sn and Zn ions are between soft and hard acids, Sn ions being softer than Zn. Se ions are classified as soft bases. This theory says that, soft acids react faster and form stronger bonds with soft bases than hard acids with soft bases, which explains the tendency to form copper selenide phases at first, then tin selenide and at the end zinc selenide phase (Lee *et al*. 2013). Moreover, the higher reactivity and relatively high mobility of copper ions with respect to zinc and tin ions help the reaction between copper and selenium ions (Zhou *et al*. 2015). At 10 minutes one can observe that many of the secondary peaks have gone, and the few present diffracted at 2 theta values of 28.1, 31.1 and 50.0° that correspond to $CuSe_2$, $Cu_{1.8}Se$ and CuSe phases respectively identified at 0 minutes, the peak at 45.3° tends to split into two peaks which can be related to the presence of secondary phases. The peaks at 27.2 and 53.8° become well defined, however one cannot associate them to a particular phase because of the diffraction of secondary, ternary and quaternary phases and due to the width of the peaks. At 20 minutes one can observe a better definition of the principal peaks at 27.2, 45.1 and 53.8°, besides the peak at 10

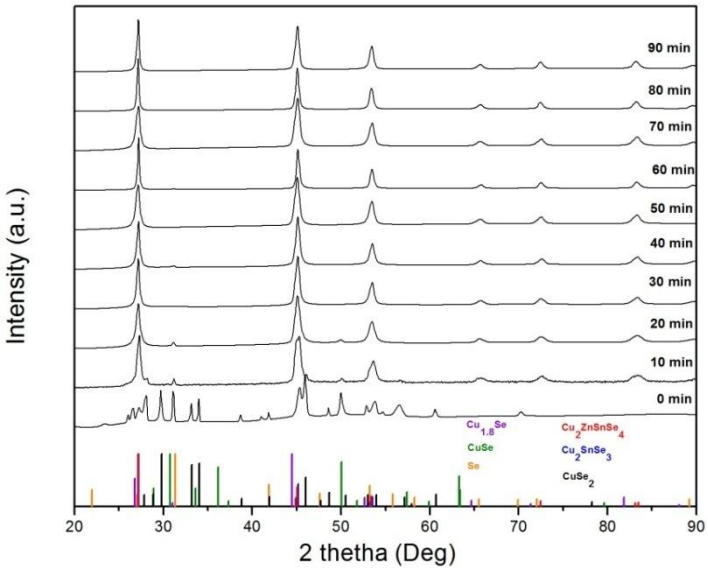

Fig. 1 XRD of nanocrystal obtained at different reaction times, from 0 to 90 minutes

minutes around 45.3° has moved to 45.1° at 20 minutes, which is characteristic of ternary and quaternary phases, besides there are still small peaks associated with the presence of $Cu_{1.8}Se$ and CuSe phases. At this time we can infer that secondary phases are almost consumed and the presence of ternary and quaternary phase becomes higher. At 30, 40 and 50 minutes apparently we can observe that there is no presence of peaks associated with secondary phases, because the peaks at 27.2, 45.1 and 53.8° indicate the presence of the ternary and quaternary phase, however it is not possible to determine clearly the phases because of the overlap of the peak patterns, moreover these peaks are wide which indicate the possibility of presence of $Cu_{1.8}Se$ and Se. On the other hand we can observe that the peak at 45.1° is higher than the peak at 27.2°, relation that changes at 60 minutes. At 60 minutes the peaks at 27.2, 45.1 and 53.8° are narrower than those at smaller times, this indicates that the quaternary phase is formed and there is no presence of secondary phases, the peaks diffracted at 2 theta values of 27.1, 45.1, 53.5, 65.5, 65.8, 72.5 and 83.4° correspond to (112), (204), (312), (400/008), (316) and (228) planes of $Cu_2ZnSnSe_4$ (PDF 00-052-0868). The observed doublet peak (400/008) indicates that the CZTSe adopts the stannite structure (space group $I\bar{4}2$ m) (Li *et al*. 2011), the ternary phase cannot be discarded by XRD because of the overlap but Raman analysis confirms the pure quaternary phase (Fig. 2). After 60 minutes we can observe that the peaks at 27.1, 45.1 and 53.5° become wider, mainly the one at 45.1° which is close to the most intense pattern peak of $Cu_{1.8}Se$ at 44.5° (PDF 01-071-4324), this suggests the tendency to decompose the pure quaternary phase achieved at 60 minutes into $Cu_{1.8}Se$, Se and Cu_2SnSe_3 observed at shorter times. This quaternary decomposition is confirmed in Raman spectroscopy analysis (Fig. 2).

In Table 1, one can observe the texture coefficients of nanocrystals synthesized at reaction times from 30 to 90 minutes, which was calculated using Eq. (1), where $\boldsymbol{T_{c(hkl)}}$ is the texture coefficient of the plane (hkl), $\boldsymbol{I_{i(hkl)}}$ is the intensity of the i-th peak corresponding to the (hkl) plane, $\boldsymbol{I_{o(hkl)}}$ is the relative intensity of the plane (hkl) reported in the PDF pattern and n is the number of peaks considered for calculations. We can observe that (204) plane presents preferential orientation

Table 1 Texture coefficients of nanocrystals obtained at reaction times from 30 to 90 minutes

Time (min)	*Tc* (112)	*Tc* (204)	*Tc* (312)
30	0.47	1.29	1.24
40	0.45	1.31	1.24
50	0.41	1.26	1.32
60	0.59	1.22	1.19
70	0.42	1.29	1.30
80	0.56	1.21	1.23
90	0.53	1.20	1.28

in all the cases, the highest value for (112) plane is observed at 60 minutes while at the same time (204) and (312) planes presents their lowest values which is related with crystallinity observed in XRD. At longer times than 60 minutes the values tend to be similar compared to times shorter than 60 minutes. This indicates that times longer than 60 minutes change the crystallinity obtained at 60 minutes, indicating a possible decomposition of crystals achieved at 60 minutes.

$$Tc(\mathrm{hkl}) = \frac{\frac{Ii(hkl)}{I0(hkl)}}{\frac{1}{n}\sum_{i=1}^{n}\frac{Ii(hkl)}{I0(hkl)}} \quad (1)$$

Lattice parameters of the sample synthesized in 60 minutes were calculated using the relation $d_{hkl} = \lambda/(2\sin\theta)$ (Bragg's law) and Eq. (2) from the data obtained by XRD. Here $\boldsymbol{h}$, $\boldsymbol{k}$ and $\boldsymbol{l}$ are Miller indices; a, b and c are the lattice parameters (in a tetragonal system $a = b \neq c$) and $\boldsymbol{d_{(hkl)}}$ is the interplanar spacing between the crystal planes (hkl). The estimated lattice parameters are found to be a = 5.692 and c = 11.312 Å. The estimated values are in good agreement with the standard values (a = 5.693 and c = 11.333 Å) reported in PDF# 052-0868.

$$\frac{1}{d^2} = \frac{h^2 + k^2}{a^2} + \frac{l^2}{c^2} \quad (2)$$

In order to confirm the phases detected in XRD analysis, we performed Raman spectroscopy. In Fig. 2 it can be observed the phases detected at reaction times from 0 to 90 minutes. At 0 minutes, we can observe the presence of the secondary phases $Cu_{1.8}Se$, $CuSe_2$ and CuSe at 192, 238 and 264 cm^{-1} respectively (Quiroz *et al*. 2014, Liu *et al*. 2013, Ganchev *et al*. 2011). Moreover, selenium was detected at 234 cm^{-1} (Holubová *et al*. 2009). These phases have been previously reported in other studies and are in agreement with XRD analysis (Fig. 1). At 10 minutes it can be observed the growth of the peak for $Cu_{1.8}Se$ phase at 192 cm^{-1}, while peaks of CuSe, $CuSe_2$ and Se have been reduced, besides the peak at 192 cm^{-1} has been extended to the left indicating the presence of ternary phase at 182 cm^{-1}. This condition is confirmed in XRD analysis because of the splitting of the peak at 45.3°. At 20 minutes, it is clearer the appearance of the peak at 182 cm^{-1}, indicating the presence of ternary phase Cu_2SnSe_3 (Lee *et al*. 2013) and there is a small presence of $Cu_{1.8}Se$ phase. At 30 and 40 minutes we can observe that the peak at 182 cm^{-1} has extended sideways indicating the formation of quaternary phase at 172 and 196 cm^{-1}, however ternary phases are predominant

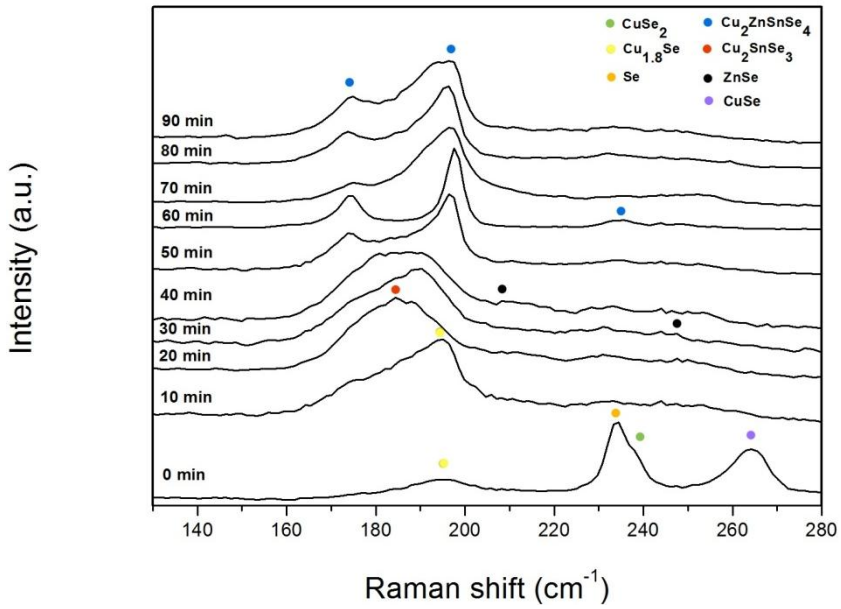

Fig. 2 Raman spectra of nanocrystal obtained at different reaction times, from 0 to 90 minutes

over quaternary phase, this condition is also observed in XRD analysis because of the width of the peak at 45.1°. Small peaks of ZnSe phase are detected at 206 and 250 cm^{-1} (Salomé *et al*. 2014). At 50 minutes, we can observe that the peak at 182 cm^{-1} has been splitted into two peaks at 173 and 196 cm^{-1}, which is clearly related to $Cu_2ZnSnSe_4$ formation and consumption of Cu_2SnSe_3 and ZnSe phases. At 60 minutes it can be observed clearly the presence of the three characteristic peaks of CZTSe phase at 173, 196 and 232 cm^{-1} (Shei and Lee 2013) with no evidence of other phases. This confirms the observed condition in XRD analysis when the peaks at 27.1, 45.1 and 53.5° are narrower than those at shorter synthesis times. After 60 minutes, we can observe that principal peak at 196 cm^{-1} becomes wider with more time, which clearly indicates the tendency for decomposition of quaternary phase into ternary and secondary phases detected at shorter synthesis times (Cu_2SnSe_3 and $Cu_{1.8}Se$). This condition is related with the widening of the peak 45.1° in XRD analysis. So we can infer that 60 minutes is the ideal time to synthesize pure CZTSe phase and that longer reaction times tends to decompose it.

4.1 Reaction mechanism

Triethanolamine plays a key role in CZTSe formation; TEA not only works as solvent but also works as reducing agent for elemental selenium (Reaction 1), activating Se to take part in reactions. Amines have probed their ability to reduce selenium when temperature increases (Lu *et al*. 2002). Besides, TEA works as a chelation agent for metallic ions (reactions 2, 3 and 4) and as a place for metallic ions and reduced selenium to meet (reactions 6, 7 and 8), reacting and forming the first secondary phases. Based on XRD and Raman spectroscopy analyses we can establish that at the beginning secondary phases CuSe and $CuSe_2$ are predominant, which is due to reaction between copper and selenium ion (reaction 5, and 8), then theses two phases tend to form the stoichiometric phase $Cu_{1.8}Se$ as can be seen in reaction 9 (where x is equal to 0.2). Then this secondary phase

reacts with SnSe to promote the formation of the ternary phase (reaction 10). Finally the ternary phase reacts with ZnSe to form the quaternary phase CZTSe. The copper deficiency (x = 0.2) is well fitted with EDS analysis reported in Table 2.

$$Se + TEA \rightarrow [Se^{2-}(TEA^{2+})] \quad (1)$$

$$Cu^{2+} + TEA \rightarrow [Cu(TEA)]^{2+} \quad (2)$$

$$Sn^{2+} + TEA \rightarrow [Sn(TEA)]^{2+} \quad (3)$$

$$Zn^{2+} + TEA \rightarrow [Zn(TEA)]^{2+} \quad (4)$$

$$Cu^{2+} + Se^{2-} \rightarrow CuSe \quad (5)$$

$$Sn^{2+} + Se^{2-} \rightarrow SnSe \quad (6)$$

$$Zn^{2+} + Se^{2-} \rightarrow ZnSe \quad (7)$$

$$CuSe + Se \leftrightarrow CuSe_2 \quad (8)$$

$$(2\text{-}x)CuSe \rightarrow Cu_{(2-x)}Se + (1\text{-}x)Se \quad (9)$$

$$Cu_{(2-x)}Se + SnSe + Se \rightarrow Cu_{(2-x)}SnSe_3 \quad (10)$$

$$Cu_{(2-x)}SnSe_3 + ZnSe \rightarrow Cu_{(2-x)}ZnSnSe_4 \quad (11)$$

Previous results indicate that the CZTSe-based best efficient solar cells have slight Cu-deficient and Zn-rich composition with Cu/(Zn+Sn) ratio oscillating between 0.8 and 1.0 and Zn/Sn from 1.0 to 1.2 (Brammertz *et al*. 2013). The EDS analysis was carried out in order to analyze the chemical composition of the samples. Table 2 shows the results obtained from nanocrystals synthesized at reaction times from 0 to 90 minutes. In these results, we can observe that Cu/(Zn+Sn) and Zn/Sn ratios decreases with the reaction time being inside the proposed ranges of

Table 2 EDS analysis of nanocrystals obtained at different reaction times from 0 to 90 minutes

Time (min)	Cu (%)	Zn (%)	Sn (%)	Se (%)	Cu/(Zn+Sn)	Zn/Sn
0	27.28	17.23	14.83	40.66	0.85	1.16
10	29.77	17.74	9.72	42.77	1.08	1.83
20	29.35	16.3	11.38	42.97	1.06	1.43
30	29.26	17.27	12.43	41.04	0.99	1.39
40	29.14	16.71	10.37	43.78	1.08	1.61
50	28.83	16.65	12.4	42.12	0.99	1.34
60	26.75	16.37	15.17	41.71	0.85	1.08
70	29.07	15.01	15.83	40.09	0.94	0.95
80	27.86	15.01	14.76	42.37	0.94	1.02
90	27.13	15.39	16.02	41.46	0.86	0.96

60 minutes, which is in agreement with XRD and Raman analyses previously reported. Besides, copper deficiency is in agreement with the value of $x = 0.2$ proposed during the reaction mechanism. Selenium content is less than the expected (50%), this might be due to a strong bonding between selenium and TEA during the chelation process, which is quite similar when oleylamine is used.

4.2 Pure CZTSe phase confirmation

In order to prove that 60 minutes was the ideal time for pure CZTSe synthesis, XPS and TEM analyses were performed. XPS analysis was carried out for CZTSe nanoparticles synthesized for 60 minutes, in order to investigate the oxidation states of the constituent elements. Figs. 3(a)-(d) show the binding energies obtained from the high-resolution core level spectra. The separation measured of 19.8 eV between the peaks of Cu 2p detected at 931.8 eV ($2p_{3/2}$) and 951.4 eV ($2p_{1/2}$) is characteristic of the presence of Cu as Cu^{+} (Fig. 3(a)). The separation measured of 23 eV between the peaks of Zn 2p detected at 1021.6 eV ($2p_{3/2}$) and 1044.6 eV ($2p_{1/2}$) is related to the presence of Zn as Zn^{2+} (Fig. 3(b)). Sn is detected as Sn^{+4} due to the presence of Sn 3d peaks at 486.1 eV ($3d_{5/2}$) and 494.5 eV ($3d_{3/2}$). 8.4 eV is the separation measured in Fig. 3(c). Se as Se^{-2} can be attributed due to the presence of two peaks located at 53.51 eV ($3d_{5/2}$) and 54.57 eV ($3d_{3/2}$) as can be observed in Fig. 3(d). The oxidation states detected are characteristic of these elements in CZTSe (Lee *et al*. 2014).

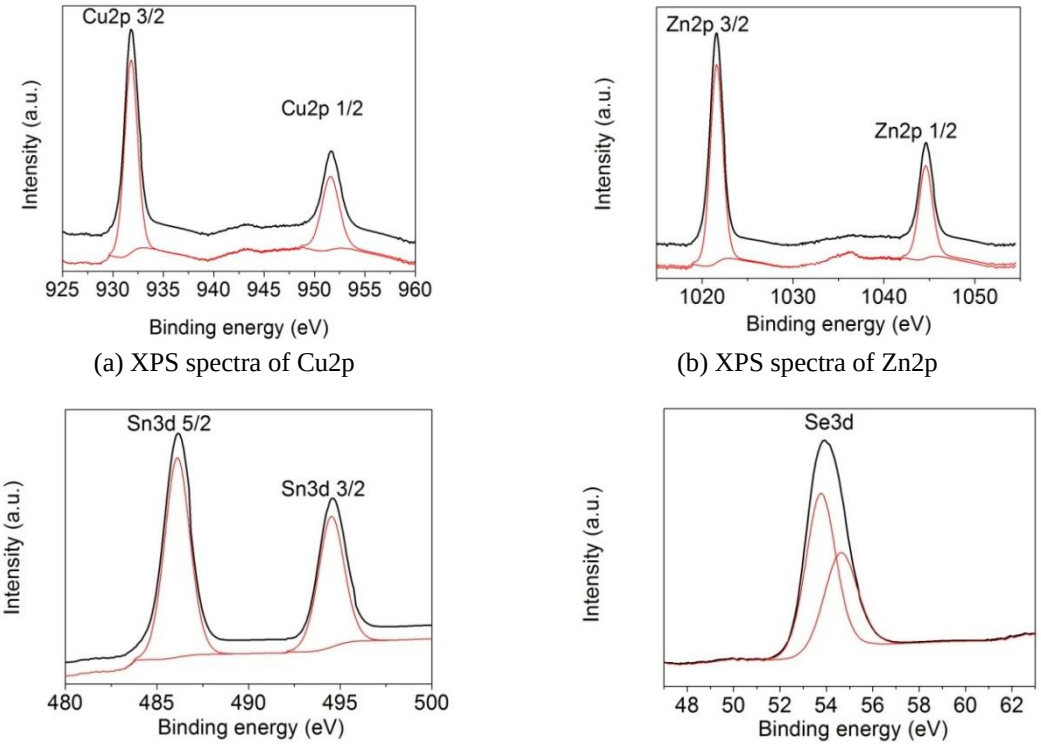

(a) XPS spectra of Cu2p (b) XPS spectra of Zn2p

(c) XPS spectra of Sn3d (d) XPS spectra of Se3d

Fig. 3 XPS spectra of CZTSe nanocrystals obtained at reaction time of 60 minutes

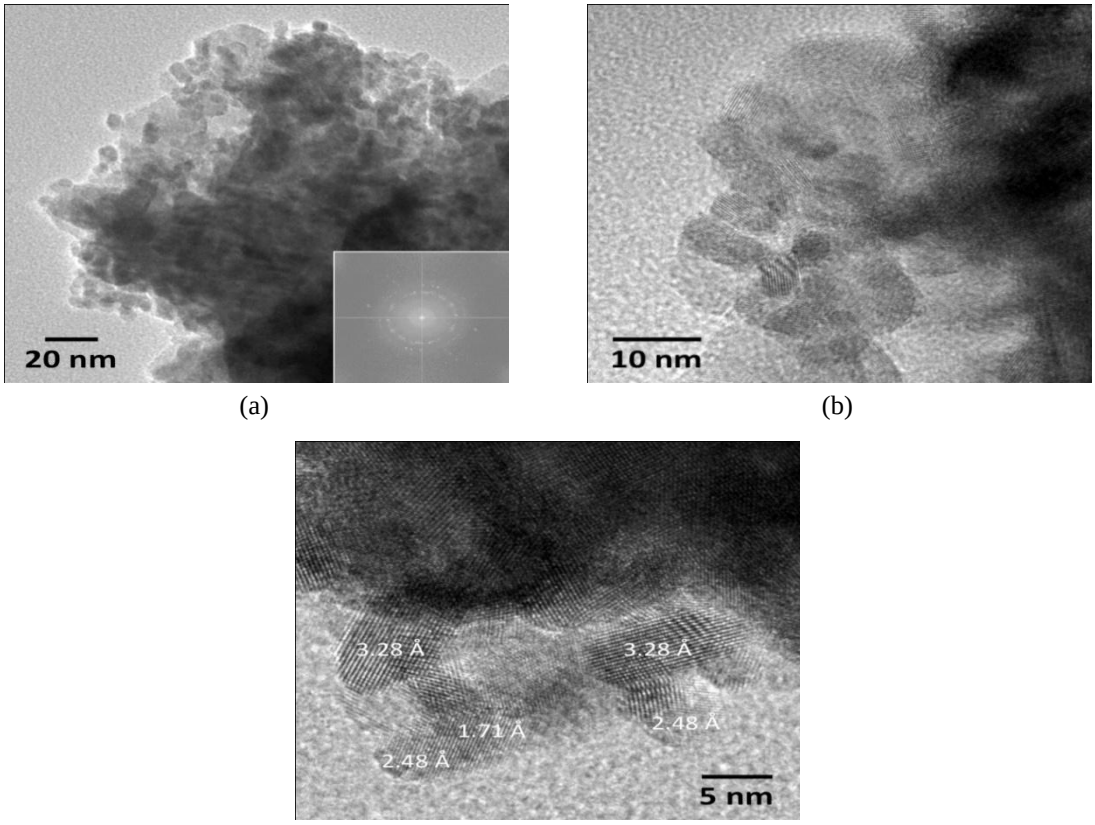

(a) (b)

(c)

Fig. 4 (a) Low magnification TEM image; (b) and (c) high magnification TEM images of CZTSe nanocrystals obtained at reaction time of 60 minutes

Nanoparticles of 6 and 8 nm were detected in low-magnification TEM image (Fig. 4(a)), which are quite similar to that synthesized in oleylamine (Rath *et al*. 2012), but smaller than that in other solvents (Du *et al*. 2012, Lee *et al*. 2013). The small particle size is related to the strong boding between selenium and amine during chelation and reduction process. Inset of Fig. 4(a) it can be observed the electron diffraction pattern in which diffraction rings are localized at 5.1, 3.3, 2.9, 2.5 and 2.0 Å, which nicely match the (101), (112), (200), (211) and (204) crystallographic planes of $Cu_2ZnSnSe_4$. The crystallinity of the nanoparticles and the homogeneity of their size are nicely seen in high-resolution TEM image shown in Fig. 4(b). Fig. 4(c) HRTEM shows a good size distribution and suitable crystallinity, the lattice fringes at 3.28, 2.48 and 1.71 Å are indicated in the figure, which correspond to the (112), (211) and (312) crystallographic planes respectively of stannite-type $Cu_2ZnSnSe_4$ detected in XRD analysis (Li *et al*. 2011).

4. Conclusions

We have observed and proposed a reaction mechanism for CZTSe synthesis by MACS trough XRD and Raman spectroscopy. The process begins with the reduction of elemental selenium and

chelation of metallic ions, which after 10 minutes produces the selenide secondary phases. Between 20 to 40 minutes ternary phase Cu_2SnSe_3 is predominant. Quaternary phase $Cu_2ZnSnSe_4$ appears clearly at 50 minutes but pure quaternary phase is achieved at 60 minutes, besides EDS analysis probes the appropriate composition. After 60 minutes the quaternary phase tends to decompose to secondary and ternary phases.

Acknowledgments

JL is Serra Húnter Fellow and is grateful to ICREA Academia program. Odin Reyes and Monica Sanchez acknowledge the CONACYT doctoral fellowships. The authors acknowledge the technical help received from Jose Campos for SEM analysis, Dra. Patricia Altuzar Coello for XRD analysis, Oscar Gómez-Daza and Pedro Fitz for general assistance. This work was funded through the project, CONACYT 236978.

References

Ahmadi, M., Pramana, S.S., Xi, L., Boothroyd, C., Lam, Y.M. and Mhaisalkar, S. (2012), Evolution pathway of CIGSe nanocrystals for solar cell applications", *J. Phys. Chem. C*, **116**(14), 8202-8209.

Bhattacharya, R.N., Batchelor, W., Granata, J.E., Hasoon, F., Wiesner, H., Ramanathan, K. and Noufi, R.N. (1998), "CuIn 1− x Ga x Se 2-based photovoltaic cells from electrodeposited and chemical bath deposited precursors", *Solar Energy Mater. Solar Cells*, **55**(1), 83-94.

Brammertz, G., Buffière, M., Oueslati, S., ElAnzeery, H., Messaoud, K.B., Sahayaraj, S. and Poortmans, J. (2013), "Characterization of defects in 9.7% efficient $Cu_2ZnSnSe_4$-CdS-ZnO solar cells", *Appl. Phys. Lett.*, **103**(16), 163904.

Du, Y.F., Zhou, W.H., Zhou, Y.L., Li, P.W., Fan, J.Q., He, J.J. and Wu, S.X. (2012), "Solvothermal synthesis and characterization of quaternary $Cu_2ZnSnSe_4$ particles", *Mater. Sci. Semicon. Process.*, **15**(2), 214-217.

Flynn, B., Wang, W., Chang, C.H. and Herman, G.S. (2012), "Microwave assisted synthesis of Cu_2ZnSnS_4 colloidal nanoparticle inks", *Physica Status Solidi* (*a*), **209**(11), 2186-2194.

Ganchev, M., Iljina, J., Kaupmees, L., Raadik, T., Volobujeva, O., Mere, A. and Mellikov, E. (2011), "Phase composition of selenized $Cu_2ZnSnSe_4$ thin films determined by X-ray diffraction and Raman spectroscopy", *Thin Solid Films*, **519**(21), 7394-7398.

Gardner, J.S., Shurdha, E., Wang, C., Lau, L.D., Rodriguez, R.G. and Pak, J.J. (2008), "Rapid synthesis and size control of $CuInS_2$ semi-conductor nanoparticles using microwave irradiation", *J. Nanopart. Res.*, **10**(4), 633-641.

Grisaru, H., Palchik, O., Gedanken, A., Palchik, V., Slifkin, M.A. and Weiss, A.M. (2003), "Microwave-assisted polyol synthesis of $CuInTe_2$ and $CuInSe_2$ nanoparticles", *Inorganic Chem.*, **42**(22), 7148-7155.

Holubová, J., Černošek, Z. and Černošková, E. (2009), "The selenium based chalcogenide glasses with low content of As and Sb: DSC, StepScan DSC and Raman spectroscopy study", *J. Non-Crystal. Solids*, **355**(37), 2050-2053.

Jackson, P., Wuerz, R., Hariskos, D., Lotter, E., Witte, W. and Powalla, M. (2016), "Effects of heavy alkali elements in Cu (In, Ga) Se2 solar cells with efficiencies up to 22.6%", *Physica Status Solidi* (*RRL*)-*Rapid Res. Lett.*, **10**(8), 583-586.

Jeon, M., Tanaka, Y., Shimizu, T. and Shingubara, S. (2011), "Formation and characterization of single-step electrodeposited Cu_2ZnSnS_4 thin films: Effect of complexing agent volume", *Energy Procedia*, **10**, 255-260.

Lee, P.Y., Shei, S.C. and Chang, S.J. (2013), "Evolution pathways for the formation of Nano-$Cu_2ZnSnSe_4$ absorber materials via elemental sources and isophorondiamine chelation", *J. Alloys Compounds*, **574**, 27-

32.
Lee, P.Y., Chang, S.P., Hsu, E.H. and Chang, S.J. (2014), "Synthesis of CZTSe nanoink via a facile one-pot heating route based on polyetheramine chelation", *Solar Energy Mater. Solar Cells*, **128**, 156-165.
Li, Z.Q., Shi, J.H., Liu, Q.Q., Chen, Y.W., Sun, Z., Yang, Z. and Huang, S.M. (2011), "Large-scale growth of $Cu_2ZnSnSe_4$ and $Cu_2ZnSnSe_4$/Cu_2ZnSnS_4 core/shell nanowires", *Nanotechnology*, **22**(26), 265615.
Liu, W., Wu, M., Yan, L., Zhou, R., Si, S., Zhang, S. and Zhang, Q. (2011), "Noninjection synthesis and characterization of $Cu_2ZnSnSe_4$ nanocrystals in triethanolamine reaction media", *Mater. Lett.*, **65**(17), 2554-2557.
Liu, T., Jin, Z., Li, J., Wang, J., Wang, D., Lai, J. and Du, H. (2013), "Monodispersed octahedral-shaped pyrite CuSe 2 particles by polyol solution chemical synthesis", *CrystEngComm*, **15**(44), 8903-8906.
Lu, J., Xie, Y., Xu, F. and Zhu, L. (2002), "Study of the dissolution behavior of selenium and tellurium in different solvents—a novel route to Se, Te tubular bulk single crystals", *J. Mater. Chem.*, **12**(9), 2755-2761.
Mitzi, D.B., Gunawan, O., Todorov, T.K., Wang, K. and Guha, S. (2011), "The path towards a high-performance solution-processed kesterite solar cell", *Solar Energy Mater. Solar Cells*, **95**(6), 1421-1436.
Panda, A.B., Glaspell, G. and El-Shall, M.S. (2006), "Microwave synthesis of highly aligned ultra-narrow semiconductor rods and wires", *J. Am. Chem. Soc.*, **128**(9), 2790-2791.
Qian, H., Qiu, X., Li, L. and Ren, J. (2006), "Microwave-assisted aqueous synthesis: a rapid approach to prepare highly luminescent ZnSe (S) alloyed quantum dots", *J. Phys. Chem. B*, **110**(18), 9034-9040.
Qin-Miao, C., Zhen-Qing, L., Yi, N., Shu-Yi, C. and Xiao-Ming, D. (2012), "Doctor-bladed Cu_2ZnSnS_4 light absorption layer for low-cost solar cell application", *Chinese Physics B*, **21**(3), 038401.
Quiroz, H.P., Seña, N.J. and Dussan, A. (2014), "Microstructural and morphological properties of nanocrystalline Cu2ZnSnSe4 thin films: Identification new phase on structure", *J. Phys.: Conference Series*, **480**(1), p. 012002.
Rath, T., Haas, W., Pein, A., Saf, R., Maier, E., Kunert, B. and Trimmel, G. (2012), "Synthesis and characterization of copper zinc tin chalcogenide nanoparticles: influence of reactants on the chemical composition", *Solar Energy Materials and Solar Cells*, **101**, 87-94.
Roe, F.J.C., Grant, G.A. and Millican, D.M. (1967), "Carcinogenicity of hydrazine and 1, 1-dimethylhydrazine for mouse lung", *Nature*, **216**(5113), 375-376.
Salomé, P.M., Fernandes, P.A., Leitão, J.P., Sousa, M.G., Teixeira, J.P. and da Cunha, A.F. (2014), "Secondary crystalline phases identification in $Cu_2ZnSnSe_4$ thin films: Contributions from Raman scattering and photoluminescence", *J. Mater. Sci.*, **49**(21), 7425-7436.
Shao, L., Zhang, J., Zou, C. and Xie, W. (2012), "$Cu_2ZnSnSe_4$ thin films by selenization of simultaneously evaporated Sn-Zn-Cu metallic lays for photovoltaic applications", *Phys. Procedia*, **32**, 640-644.
Shei, S.C. and Lee, P.Y. (2013), "Synthesis of CZTSe nanocrystal prepared by a facile route in coordinating solvent from elemental sources", *Nanotechnology, IEEE Transactions on*, **12**(4), 532-538.
Shockley, W. and Queisser, H.J. (1961), "Detailed balance limit of efficiency of p-n junction solar cells", *J. Appl. Phys.*, **32**(3), 510-519.
Shyju, T.S., Anandhi, S., Suriakarthick, R., Gopalakrishnan, R. and Kuppusami, P. (2015), "Mechano-synthesis, deposition and characterization of CZTS and CZTSe materials for solar cell applications", *J. Solid State Chem.*, **227**, 165-177.
Todorov, T.K., Reuter, K.B. and Mitzi, D.B. (2010), "High-efficiency solar cell with earth-abundant liquid processed absorber", *Adv. Mater.*, **22**(20), 156-159.
Vallejo, O.R., Sánchez, M., Pal, M., Espinal, R., Llorca, J. and Sebastian, P.J. (2016), "Synthesis and characterization of nanoparticles of CZTSe by microwave-assited chemical synthesis", *Mater. Res. Express*, **3**(12), 125017.
Wang, Y., Ai, X., Miller, D., Rice, P., Topuria, T., Krupp, L. and Song, Q. (2012), "Two-phase microwave-assisted synthesis of Cu 2 S nanocrystals", *CrystEngComm*, **14**(22), 7560-7562.
Wang, W., Winkler, M.T., Gunawan, O., Gokmen, T., Todorov, T.K., Zhu, Y. and Mitzi, D.B. (2014), "Device characteristics of CZTSSe thin-film solar cells with 12.6% efficiency", *Adv. Energy Mater.*, **4**(7),

1301465.

Wangperawong, A., King, J.S., Herron, S.M., Tran, B.P., Pangan-Okimoto, K. and Bent, S.F. (2011), "Aqueous bath process for deposition of Cu_2ZnSnS_4 photovoltaic absorbers", *Thin Solid Films*, **519**(8), 2488-2492.

Washington Ii, A.L. and Strouse, G.F. (2008), "Microwave synthesis of CdSe and CdTe nanocrystals in nonabsorbing alkanes", *J. Am. Chem. Soc.*, **130**(28), 8916-8922.

Wibowo, R.A., Jung, W.H. and Kim, K.H. (2010), "Synthesis of $Cu_2ZnSnSe_4$ compound powders by solid state reaction using elemental powders", *J. Phys. Chem. Solids*, **71**(12), 1702-1706.

Zhou, J., You, L., Yi, Q. and Ye, Z. (2013), "One-step synthesis of $Cu_2ZnSnSe_4$ microparticles via a facile solution route in triethylenetetramine reaction media and its characterization", *Mater. Lett.*, **107**, 225-227.

Zhou, B., Xia, D. and Wang, Y. (2015), "Phase-selective synthesis and formation mechanism of CZTS nanocrystals", *RSC Advances*, **5**(86), 70117-70126.

Zoppi, G., Forbes, I., Miles, R.W., Dale, P.J., Scragg, J.J. and Peter, L.M. (2009), "$Cu_2ZnSnSe_4$ thin film solar cells produced by selenisation of magnetron sputtered precursors", *Prog. Photovoltaics: Res. Appl.*, **17**(5), 315-319.